JOURNAL OF Applied Polymer SCIENCE

Viscoelastic Properties and Extrusion Processability of Poly(vinyl butyral)

Sunatda Arayachukiat, Monchai Siriprumpoonthum, Shogo Nobukawa, Masayuki Yamaguchi
School of Materials Science, Japan Advanced Institute of Science and Technology, 1-1 Asahidai, Nomi, Ishikawa 923-1292, Japan
Correspondence to: M. Yamaguchi (E-mail: m_yama@jaist.ac.jp)

ABSTRACT: Rheological properties and flow instability at capillary extrusion of a random terpolymer composed of vinyl butyral, vinyl alcohol, and vinyl acetate, that is denoted as PVB in this article, are studied. It is found that the rubbery plateau modulus G_N^0 is 1.3 MPa at 100°C from the oscillatory shear modulus. Furthermore, the average molecular weight between entanglement couplings M_e is found to be 2670. Because of the relatively high value of G_N^0, it shows rubbery region in the wide temperature range (90°C–180°C). At the capillary extrusion, the surface instability (shark-skin failure) appears prior to volumetric melt fracture. The onset stress of the shark-skin failure, ca. 0.18 MPa, is similar to that of polyethylene, although PVB used in this study has narrow molecular weight distribution. Moreover, the apparent slippage is not detected, presumably due to good adhesion to the die wall. © 2014 Wiley Periodicals, Inc. J. Appl. Polym. Sci. **2014**, *131*, 40337.

KEYWORDS: rheology; extrusion; viscoelastic properties; flow instability

Received 15 June 2013; accepted 19 December 2013
DOI: 10.1002/app.40337

INTRODUCTION

Poly(vinyl butyral), a derivative of poly(vinyl alcohol) (PVA), is widely used in laminated safety glasses, paints, adhesives, and a binder for ceramics, because of the good adhesive strength to glasses, ceramics, and metals. It is prepared by reacting PVA with butyraldehyde (BA) in the presence of an acid catalyst, in which the hydroxyl groups in PVA react with BA to form 1,3-dioxane, that is, acetal, rings. The compositions of vinyl alcohol (VA) and BA are determined by the reaction condition. Furthermore, it usually contains a small amount of vinyl acetate (VAc), since PVA is prepared from poly(vinyl acetate). Therefore, the polymer is actually a random terpolymer comprising of VB, VA, and VAc, as shown in Figure 1, although it is conventionally called "poly(vinyl butyral)" in not only industries but also academia. In this article, "PVB" is used to express the terpolymer following the conventional way.

The molecular characteristics of PVB have been studied mainly by thermal analysis[1,2] and dilute solution properties such as size exclusion chromatography[3,4] and nuclear magnetic resonance.[1,5] According to them, the random structure of PVB results in an amorphous polymer with no discernible crystallinity except the polymers having high VA content (more than 63.3 wt %).[1] It was also found that the glass transition temperature T_g increases and the thermal stability decreases, as increasing the VA content.[1,2] Furthermore, Morais et al. evaluated the surface tension which is an important property for the PVB applications.[6]

Blends with other polymeric materials have been also studied greatly. Because PVB contains both hydrophilic and hydrophobic parts in the structure, it can be miscible/compatible with both hydrophilic and hydrophobic polymers. In fact, several researchers have reported on the miscibility and/or compatibility with various polymers such as polyamide,[7,8] poly(ε-caprolactone),[9–11] poly(butylene terephthalate),[12] polyurethane,[13] poly(ethylene glycol),[14] poly(vinyl chloride),[15] poly(methyl methacrylate),[16] cellulose acetate,[17] and poly(3-hydroxybutyrate).[18] In particular, advanced studies on the miscibility considering the effect of copolymerization, that is, strong unfavorable interaction between the commoner units, have provided the new concept for a material design of polymer blends.[7,11,12,16,18,19]

As compared with the studies on the blends with other polymers, the rheological properties and mechanical properties of pure PVB have not been studied so much at the best of our knowledge. One of the reasons will be the restricted applications of PVB as mentioned before. However, due to the increase in the attention to the global environment, PVB collected from laminated glasses is used as a recycled resin recently, especially in the automobile industry.[20] Therefore, further studies on the rheological properties are inevitable by the following reasons:

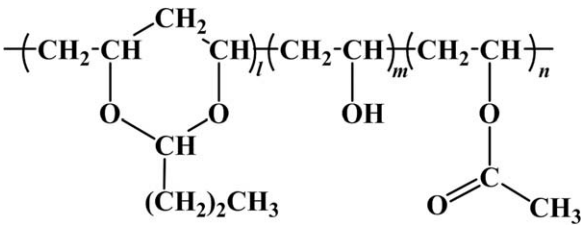

Figure 1. Chemical structure of PVB.

(1) morphology in an immiscible blend is strongly affected by the rheological properties, (2) rheological properties in the molten state decides the molecular orientation, and thus, the mechanical anisotropy in the solid state, and (3) flow instability at processing operations is mainly determined by the rheological properties. Of course, the study on the processability is considerably important to widen the application of the recycled PVB.

In this article, therefore, rheological characterization of PVB is carried out by linear viscoelastic measurements. Furthermore, the evaluation of extrusion properties including the onset of flow instabilities is performed in detail using a capillary rheometer.

EXPERIMENTAL

Material

The polymer used in this study, denoted as PVB, was a terpolymer composed of vinyl butyral (80 wt %, 57 mol %), VA (18 wt %, 41 mol %), and VAc (2 wt %, 2 mol %) produced by Denki Kagaku Kogyo, Japan (Denka PVB 4000-4). The molecular weight of the sample was determined by simultaneous measurements of multiangle light scattering (Wyatt Technology, Dawn Heleos) and gel permeation chromatography (Tosoh, HLC-8120GPC, Japan) with TSKgel GMHHR-H (Tosoh). Tetrahydrofuran was used as an eluent at a flow rate of 1.0 mL/min at 40°C, and the sample concentration was 1.0 mg/mL. The number-, weight-, and *z*-average molecular weights were 8.4×10^4, 1.5×10^5, and 2.8×10^5, respectively.

The sample was compressed into flat sheets by a compression-molding machine (Tester Sangyo, Table-type test-press, Japan) at 190°C under 10 MPa for 3 min. Then, the samples were rapidly cooled down in an ice-water bath.

Measurements

Temperature dependence of oscillatory tensile moduli such as storage modulus E', loss modulus E'', and loss tangent tan δ was measured at 10 Hz from 0°C to 200°C by a dynamic mechanical analyzer (UBM, E-4000, Japan) using a rectangular specimen with 5 mm in width and 20 mm in length. The heating rate was 2°C/min.

Frequency dependence of the oscillatory shear moduli such as storage modulus G' and loss modulus G'' was measured in the temperature range from 100°C to 250°C by a rotational-type rheometer (TA Instruments, AR2000) using a parallel plate geometry. The measurements were carried out under a nitrogen atmosphere in order to avoid thermo-oxidative degradation. The time–temperature superposition was applied to the frequency dependence of oscillatory moduli at different temperatures in an attempt to determine the linear viscoelastic properties over a wide range of time scales.

Capillary extrusion was performed by a pressure-driven capillary rheometer (Yasuda Seiki Seisakusyo, 140 SAS-2002, Japan) at 190°C, 220°C, and 250°C to evaluate the steady-state shear viscosity and the appearance of extruded strands. The molten polymer was extruded through a circular die having the following dimension: 1 mm of the diameter, 10 mm of the length, and the entrance angle of 180°. The Bagley and Rabinowitch corrections were not carried out in this study. The extruded strand was observed by a stereomicroscope (Leica, S6E, Germany). Furthermore, the magnified surface images were collected for some strands using a scanning electron microscope (SEM) (Hitachi, S400, Japan) with an acceleration voltage of 20 kV. An ion sputtering machine (Hitachi, E1010, Japan) was used to coat non-conducting specimens with Pt/Pd.

Density was measured by a buoyancy method using a chemical balance. Silicone oil at 100°C (900.8 kg/m^3) was used as a liquid.

RESULTS AND DISCUSSION

Linear Viscoelastic Properties

Figure 2 shows the temperature dependence of dynamic tensile modulus at 10 Hz. As demonstrated by a peak of the loss modulus E'' and an abrupt drop of the storage modulus E', the glass transition temperature T_g is found to be located around at 80°C. It should be noted that the rubbery region is observed in the wide temperature range with a relatively high modulus. In general, conventional amorphous plastics do not show such a wide temperature range of rubbery region without crystalline parts. Otherwise, severe problems due to high viscosity occur at various processing operations. The broad range of rubbery region is attributed to a large amount of entanglement couplings per a chain not due to the fringed micelle structure like poly(vinyl chloride),[21] in which crystalline parts with high T_m act as crosslink points. This is reasonable because PVB does not

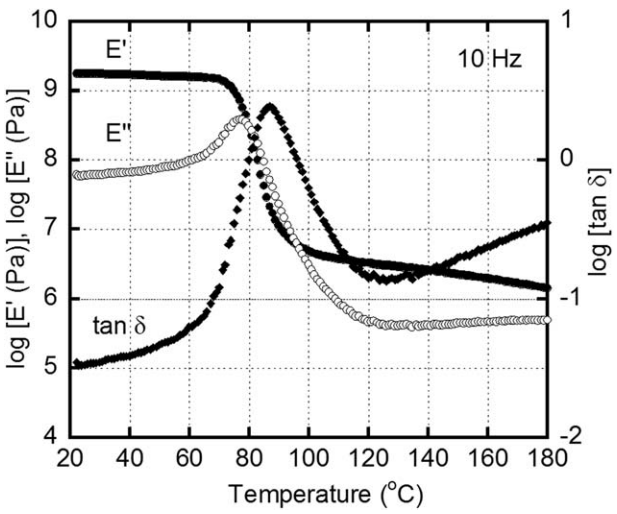

Figure 2. Temperature dependence of (*closed circle*) tensile storage modulus E', (*open circle*) loss modulus E'', and (*closed diamond*) loss tangent tan δ at 10 Hz.

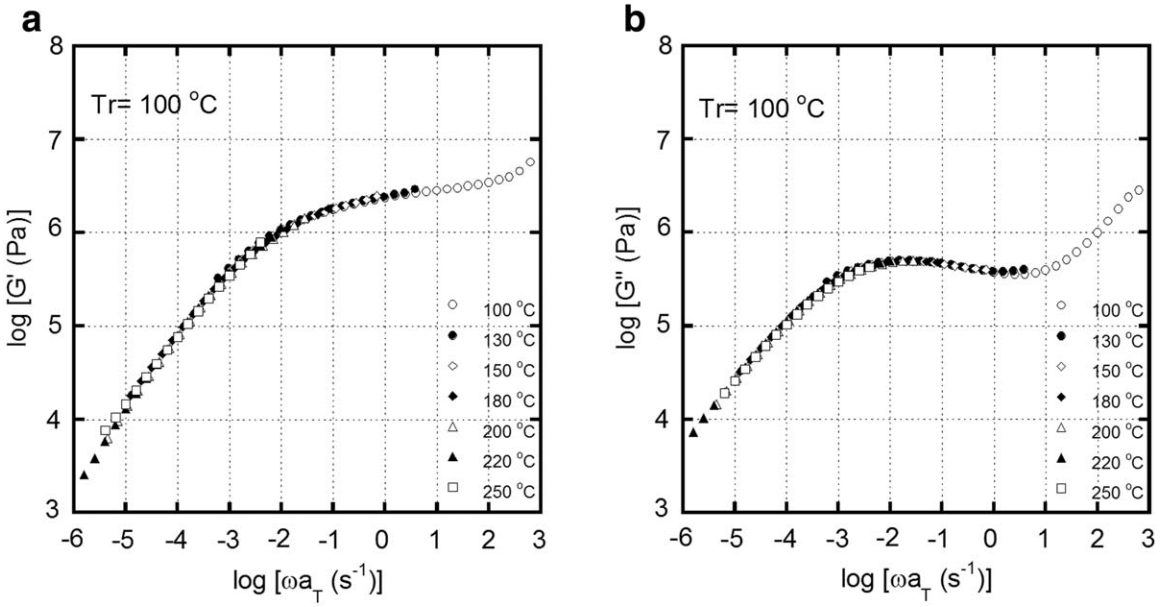

Figure 3. Master curves of frequency dependence of oscillatory shear moduli such as (**a**) storage modulus G' and (**b**) loss modulus G'' at 100°C as a reference temperature: (*open circle*) 100°C, (*closed circle*) 130°C, (*open diamond*) 150°C, (*closed diamond*) 180°C, (*open triangle*) 200°C, (*closed triangle*) 220°C, and (*open square*) 250°C.

have any crystallinity.[1,2] This was confirmed also for the present sample by means of the differential scanning calorimetry and wide-angle X-ray diffraction pattern (but not presented here).

Figure 3 shows the master curves of frequency dependence of oscillatory shear moduli such as storage modulus G' and loss modulus G''. The reference temperature is 100°C (the temperature at the density measurement). The curves cover the terminal and rubbery zones in the frequency range. Apparently, the time–temperature superposition principle is applicable to the polymer.[22] The shift factor a_T is expressed by the following WLF equation[23] as shown in Figure 4.

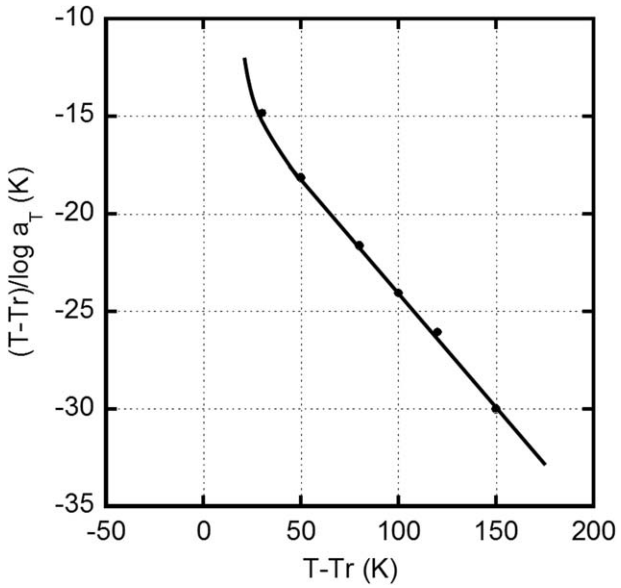

Figure 4. Relation between $T - T_r$ and $(T - T_r)/\log a_T$.

$$\log a_T = -\frac{c_1(T-T_r)}{c_2+T-T_r} \quad (1)$$

The shift factors also obey the Arrhenius-type relation (Andrade equation) beyond 150°C. The apparent flow activation energy beyond 150°C is calculated to be 52.9 kJ/mol.

Since the polymer has a relatively narrow molecular weight distribution ($M_w/M_n = 1.72$), the G'' curve shows a clear peak, that is, narrow distribution of relaxation time, around at $10^{-1}-10^{-3}$/s. The rubbery plateau modulus G_N^0 is evaluated by the following equation,[23]

$$G_N^0 = \frac{2}{\pi}\int_{-\infty}^{a} G'' \, d\ln\omega \quad (2)$$

where a is the upper limit before the transition zone is entered.

In this study, the G'' versus ln ω curve is numerically integrated from ln $\omega = -\infty$ to the maximum of G'', and the result was doubled. Consequently, G_N^0 is calculated to be 1.3 MPa at 100°C.

It is well known that the average molecular weight between entanglement couplings (M_e) is inversely proportional to G_N^0 as,

$$M_e = \frac{\rho RT}{G_N^0} \quad (3)$$

where ρ is the density and R is the gas constant.[23]

Since the density at 100°C is found to be 1118.1 kg/m^3 by the buoyancy method, M_e is calculated to be 2670. Considering that the time range of the rubbery plateau region for the relaxation modulus is proportional to $(M/M_e)^{3.4}$, the low value of M_e, that is, large number of M/M_e, provides the rubbery plateau modulus in the long time scale.[24] This is reasonable because one chain has a lot of entanglement couplings by points. Moreover, based on the time–temperature superposition principle, this is

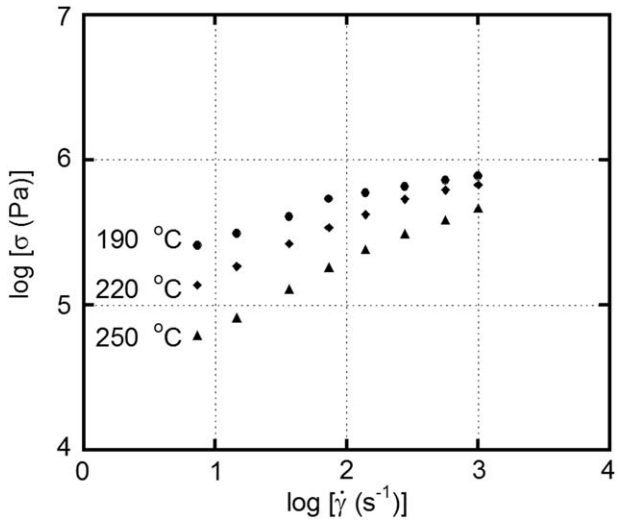

Figure 5. Shear stress σ as a function of shear rate $\dot{\gamma}$ at (*circle*) 190°C, (*diamond*) 220°C, and (*triangle*) 250°C.

responsible for the wide temperature range of the rubbery plateau region (90°C–180°C) for the oscillatory modulus. Furthermore, the value is considerably smaller than that of poly(vinyl acetate) ($M_e = 8500$).[25] In case of PVA, the critical molecular weight ($\cong 2M_e$) is known to be 5300–7500.[26,27] Because M_e of a random copolymer is between those of the homopolymers, it is predicted that poly(vinyl butyral) homopolymer has low M_e. It should be interesting to note that polysaccharides with a random-coil conformation such as cellulose, agarose, and galactomannnan have relatively low M_e,[28–30] suggesting the flexible nature of a saturated ring containing oxygen atoms.

Capillary Extrusion Properties

Figure 5 shows the flow curves at various temperatures evaluated by the capillary rheometer, and Figure 6 shows the optical micrographs observed by the stereomicroscope for the strands extruded at various shear rates and temperatures. The flow curves and the pictures indicate that the apparent slippage such as spurt flow or slip-stick failure, characterized by periodic smooth/rough regions on an extrudate, is not detected in the experimental shear rate range at any temperature. This is presumably attributed to the good adhesive strength of PVB to the die wall. Furthermore, the flow curves are not superposed onto each other by a simple horizontal shift in the high stress region, which will be owing to the gross, volumetric melt fracture.

The onset of shark-skin failure is shown by SEM images in Figure 7. The small-scale distortion is detected on the surface of the strands.

The strands obtained at 190°C show rough surface at any shear rate [Figure 7(a)], suggesting that the onset shear stress is lower than 0.256 MPa (at 7.29/s). The gross melt fracture with rough surface is detected at 72.9/s at this temperature. At higher temperatures, rough surface, that is, shark-skin failure, is detected at 0.185 MPa [14.6/s at 220°C, as shown in Figure 7(b)] and 0.182 MPa (72.9/s at 250°C). The results indicate that the onset stress of the shark-skin failure is around 0.18 MPa for PVB. The value is almost similar to that of polyethylene and slightly higher than that of polypropylene.[31]

In general, a polymer melt shows various flow instabilities at high output rate conditions, such as shark-skin failure, spurt flow, helical distortion, and gross chaotic melt fracture, which have been summarized in books and review articles.[31–35] According to Meller et al.,[36] both shark-skin failure and spurt flow occur beyond the critical shear stress at die exit, while volumetric melt fracture such as helical distortion and chaotic distortion is detected beyond the critical elongational stress at the die entrance. Recently, an interesting result was reported by Palza et al., in which they detected the origin of shark-skin failure in the die land not at die exit.[37]

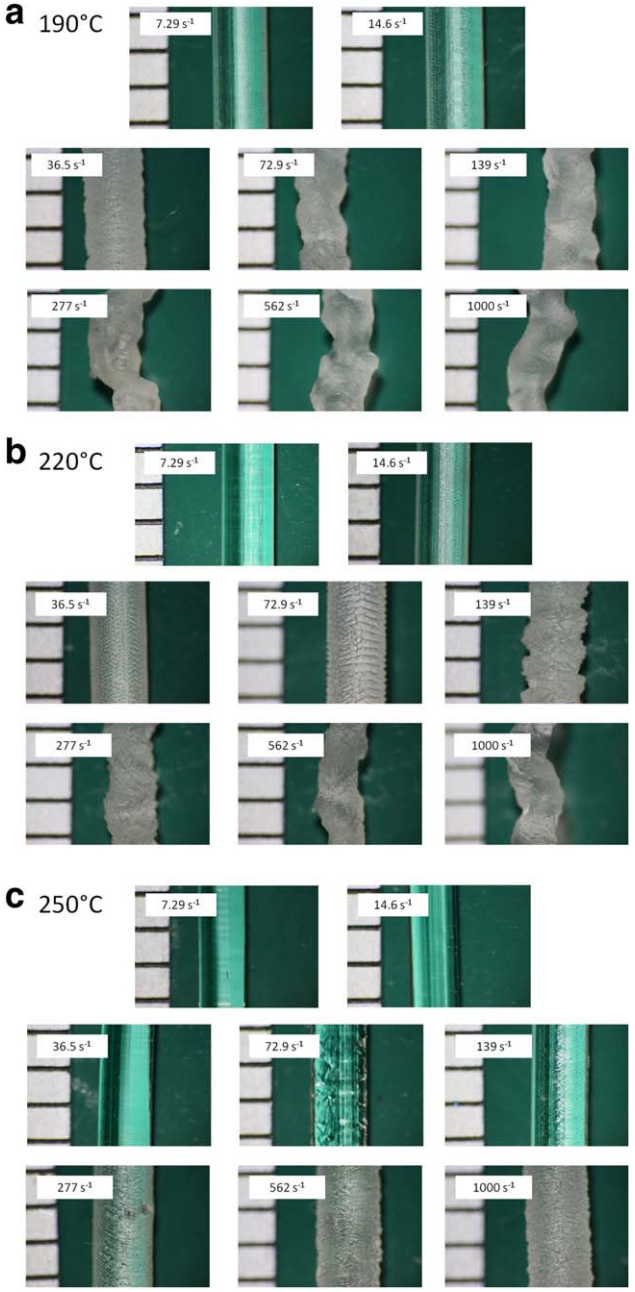

Figure 6. Photographs of strands extruded at (**a**) 190°C, (**b**) 220°C, and (**c**) 250°C at various shear rates. The distance between the neighbor lines is 1 mm. [Color figure can be viewed in the online issue, which is available at wileyonlinelibrary.com.]

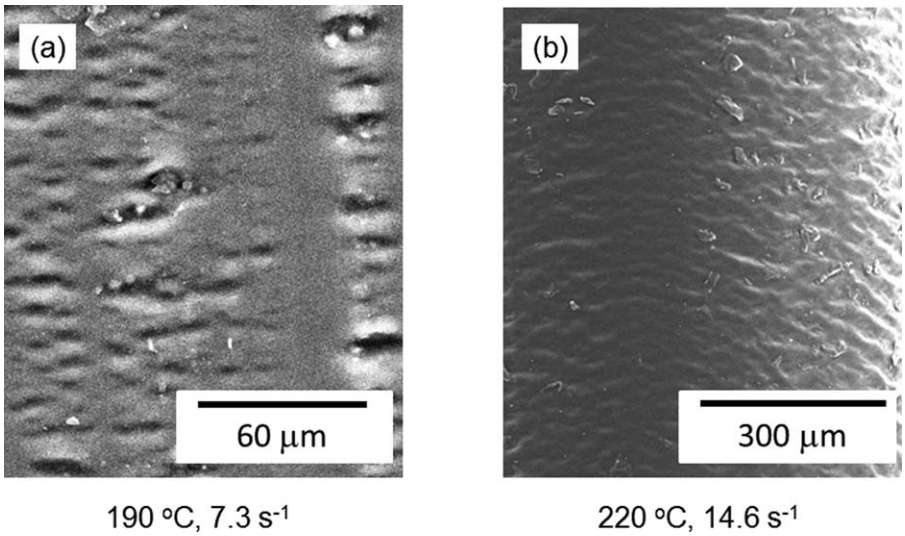

Figure 7. SEM images of the surface of strands extruded at the following conditions: (**a**) 7.29/s, 190°C and (**b**) 14.6/s, 220°C.

These flow instabilities should be seriously considered for industrial applications, because they decide the production speed. For most linear polymers such as polyethylene, polypropylene, polydimethylsiloxane, and polyisobutylene, the shark-skin failure appears prior to the other instabilities,[31–35] although it was recently demonstrated that even a long-chain branched polymer shows the shark-skin failure prior to the gross melt fracture when the melt has strong shear history.[38] Therefore, the onset of shark-skin failure has to be solved at first to increase the output rate. In the past decades, in particular, linear low-density polyethylene produced by metallocene catalyst suffers from the shark-skin failure greatly because of its narrow molecular weight distribution. The cause of the shark-skin failure has been discussed for a long time and is roughly classified into two mechanisms. According to Cogswell,[39] the discontinuity in velocity at the die exit, leading to high tensile stress, is responsible for the surface cracks appeared as a "peel-off" failure.[37] The stress at the crack-opening can be discussed referring to the failure mechanism of glassy amorphous polymers,[40–43] because of the high Deborah number condition. Another well-known mechanism leading to shark-skin failure is slippage, that is, adhesive failure, between a polymer melt and the die wall. When the debonding stress between the wall and a polymer melt is lower than the cohesive strength of the polymer melt, the melt slips on the wall. The detachment of a melt from die surface accompanied with cracks by adhesive failure leads to surface instabilities.[44] Furthermore, Brochard and de Gennes proposed the idea that slippage occurs between a polymer melt and the polymer chains adsorbed on the die wall.[45] Finally, Allal et al.[46,47] derived the onset shear stresses of the shark-skin failures ascribed to surface rupture σ_c and slippage σ_s as follows:

$$\sigma_c = \frac{1}{2} G_N^0 \frac{N_e}{\sqrt{N_0}} \tag{4}$$

$$\sigma_s = \frac{9}{4\pi} G_N^0 C_{ad} \frac{N_e}{\sqrt{N_0}} \tag{5}$$

where N_e and N_0 are the number of monomers between entanglements and the number of monomers per chain, respectively, and C_{ad} is the fraction of monomers adsorbed on the surface. As indicated in the equations, the critical stresses increase with the rubbery plateau modulus, G_N^0, which corresponds with the experimental results obtained using various types of ethylene-α-olefin copolymers.[48]

Since G_N^0 is inversely proportional to M_e, the equations can be expressed as:

$$\sigma_c = \frac{1}{2} \frac{\rho RT}{M_e} \frac{M/M_e}{\sqrt{M/M_0}} = \frac{1}{2} \rho RT M_0^{0.5} \frac{M^{0.5}}{M_e{}^2} \tag{6}$$

$$\sigma_s = \frac{9}{4\pi} \frac{\rho RT}{M_e} C_{ad} \frac{N_e}{\sqrt{N_0}} = \frac{9}{4\pi} \rho RT C_{ad} M_0^{0.5} \frac{M^{0.5}}{M_e{}^2} \tag{7}$$

where M and M_0 are the molecular weights of a chain and the monomer, respectively.

As shown in the linear viscoelastic properties, M_e (=2670) is relatively low for PVB, and thus the onset stress of the shark-skin failure must be low irrespective of the origin. The values of onset stresses at 220°C, predicted by eqs. (6) and (7), are $\sigma_c = 0.9$ MPa and $\sigma_s = 1.2 \times C_{ad}$ MPa, respectively, for the present sample. Since C_{ad} is around 0.1–0.2,[47] there is a possibility that the surface slippage is the origin of the shark-skin failure for PVB.

Although eqs. (4–7) enable to predict the onset stress for a monodispersed polymer, molecular weight distribution also has a dominant effect on the shark-skin failure. Yamaguchi et al.[48] derived the following relation for the apparent shear stress at the die wall σ using the Carreau's equation proposed for non-Newtonian liquids.[49]

$$\sigma(\dot{\gamma}) = G_N^0 f^{n-1} \mathrm{De}^{\,n} \tag{8}$$

where De is the Deborah number and f is given by the ratio of τ_w (weight-average relaxation time) to τ_n (number-average relaxation time). In the case of a linear polymer, therefore, f is determined by the molecular weight distribution.

This equation provides the information on processing failures due to the pronounced melt elasticity (high Deborah number)

including the shark-skin failure.[38,48,50,51] When a polymer melt has narrow molecular weight distribution, that is, small f, Deborah number becomes large at a constant shear stress. As a result, the melt easily shows the shark-skin failure. Since the relaxation time of the present PVB is not evaluated, the critical stress cannot be calculated quantitatively from eq. (8). However, the equation enables to discuss the onset stress considering the molecular weight distribution. In this study, M_w/M_n of the present sample is only 1.7, which is a typical value for commercialized PVB.[1,2] The value is narrower than those of most commercialized polymers. In spite of the narrow molecular weight distribution, the onset stress is not so low and similar to that of commercially available polyethylenes having broad molecular weight distribution. The result indicates that PVB intrinsically has a high level of onset shear stress for the shark-skin failure.

CONCLUSION

In the present study, the linear viscoelastic properties for a terpolymer composed of vinyl butyral (80 wt %), VA (18 wt %), and VAc (2 wt %), that is denoted as "PVB" in the article, is investigated. It is found that the polymer has a high level of rubbery plateau modulus (1.3 MPa), that is, low M_e (2670). Consequently, it shows the rubbery state in the wide temperature range. Furthermore, the flow instabilities of this polymer are examined in detail using a pressure-driven capillary rheometer with a circular die. It is found that the onset stress of shark-skin failure is around 0.18 MPa, which is almost identical to that of a conventional polyethylene and slightly higher than that of a conventional polypropylene in spite of the narrow molecular weight distribution. The low M_e is responsible for the high onset shear stress of the shark-skin failure, leading to high output rate at extrusion processing.

ACKNOWLEDGMENTS

The authors appreciate TOSOH Analysis and Research Center Co., Ltd., for their technical support of the molecular weight measurements.

REFERENCES

1. Cascone, E.; David, D. J.; Di Lorenzo, M. L.; Karasz, F. E.; Macknight, W. J.; Martuscelli, E.; Raimo, M. *J. Appl. Polym. Sci.* **2001**, *82*, 2934.
2. Fernandez, M. D.; Fernandez, M. J.; Hoces, P. *J. Appl. Polym. Sci.* **2006**, *102*, 5007.
3. Remsen, E. *J. Appl. Polym. Sci.* **1991**, *42*, 503.
4. Strigel, A. M. *Polym. Int.* **2004**, *53*, 1806.
5. Lebek, B.; Menge, H.; Schlothauer, K.; Schneider, H.; Kivayeva, L. S.; Fedotov, V. D. *Polymer* **1991**, *32*, 2335.
6. Morais, D.; Valera, T. S.; Demarquette, N. R. *Macromol. Symp.* **2006**, *245*, 208.
7. Jeong, H. K.; Rooney, M.; David, D. J.; MacKnight, W. J.; Karasz, F. E.; Kajiyama, T. *Polymer* **2000**, *41*, 6003.
8. Valera, T. S.; Demarquette, N. R. *Eur. Polym. J.* **2008**, *44*, 755.
9. Lee, J. C.; Ajima, K. N.; Ikehara, T.; Nishi, T. *J. Appl. Polym. Sci.* **1997**, *65*, 409.
10. Lee, J. C.; Ikehara, T.; Nishi, T. *J. Appl. Polym. Sci.* **1998**, *69*, 193.
11. Nozue, Y.; Kurita, R.; Hirano, S.; Kawasaki, N.; Ueno, S.; Iida, A.; Nishi, T.; Amemiya, Y. *Polymer* **2003**, *44*, 6397.
12. Tripathy, A. R.; Chen, W.; Kukureka, S. N.; MacKnight, W. J. *Polymer* **2003**, *44*, 1835.
13. Sincock, T. F.; David, D. J. *Polymer* **1992**, *33*, 4515.
14. Qiu, Y. R.; Ouyang, W. *Mater. Sci. Eng. C* **2012**, *32*, 167.
15. Peng, Y.; Sui, Y. *Desalination* **2006**, *196*, 13.
16. Chen, W.; David, D. J.; MacKnight, W. J.; Karasz, F. E. *Macromolecules* **2001**, *34*, 4277.
17. Qian, J. W.; Chen, H. L.; Zhang, L.; Qin, S. H.; Wang, M. *J. Appl. Polym. Sci.* **2002**, *83*, 2434.
18. Chen, W.; David, D. J.; MacKnight, W. J.; Karasz, F. E. *Polymer* **2001**, *42*, 8407.
19. Jeong, H. K.; Rooney, M.; David, D. J.; MacKnight, W. J.; Karasz, F. E.; Kajiyama, T. *Polymer* **2000**, *41*, 6671.
20. Tupy, M.; Merinska, D.; Kasparkova, V. Material Recycling, Trends and Perspectives; InTech: Croatia, **2012**.
21. Yamaguchi, M. *J. Appl. Polym. Sci.* **2001**, *82*, 1277.
22. Yamaguchi, M.; Wakabayashi, T. *Adv. Polym. Technol.* **2006**, *25*, 236.
23. Ferry, J. D. Viscoelastic Properties of Polymers, 3rd ed.; Wiley-Interscience: New York, **1980**.
24. Graessley, W. W. Polymeric Liquids & Networks: Dynamics and Rheology; Garland Science: London, **2008**.
25. Fetters, L. J.; Lohse, D. J.; Colby, R. H. In Physical Properties of Polymers Handbook, 2nd ed.; Mark, J. E., Ed.; Springer: Berlin, **2006**; Chapter *25*.
26. Aharoni, S. M. *Macromolecules* **1986**, *19*, 426.
27. Porter, R. S.; Johnson, J. F. *Chem. Rev.* **1966**, *66*, 1.
28. Horinaka, J.; Yasuda, R.; Takigawa, T. *J. Polym. Sci. Part B: Polym. Phys.* **2011**, *49*, 961.
29. Horinaka, J.; Yasuda, R.; Takigawa, T. *Carbohyd. Polym.* **2012**, *89*, 1018.
30. Maeda, A.; Inoue, T. *Nihon Reoroji Gakkaishi* **2011**, *39*, 159.
31. Koopmans, R.; Doelder, J.; Molenaar, J. Polymer Melt Fracture; CRC Press: Boca Raton, **2010**.
32. Piau, J. M.; Agassant, J. F. Rheology for Polymer Melt Processing; Elsevier: Amsterdam, **1996**.
33. Wang, S.-Q. *Adv. Polym. Sci.* **1999**, *138*, 227.
34. Hatzikiriakos, S. G.; Migler, K. B. Polymer Processing Instabilities; Marcel Dekker: New York, **2005**.
35. Tadmor, Z.; Gogos, C. G. Principles of Polymer Processing, 2nd ed.; Wiley-Interscience: New York, **2006**.
36. Meller, M.; Luciani, A.; Sarioglu, A.; Manson, J.-A. *Polym. Eng. Sci.*, **2002**, *42*, 611.
37. Palza, H.; Filipe, S.; Naue, I. F. C.; Wilhelm, M. *Polymer* **2010**, *51*, 522.
38. Monchai, S.; Mieda, N.; Doan, A. V.; Nobukawa, S.; Yamaguchi, M. *J. Appl. Polym. Sci.* **2012**, *124*, 429.
39. Cogswell, F. N. Polymer Melt Rheology; George Godwin: London, **1981**.
40. Kambour, R. P. *J. Polym. Sci. Macro. Rev.* **1973**, *7*, 1.

41. Kausch, H. H. Polymer Fracture; Springer-Verlag: Berlin, **1978**; Chapter *9*.
42. Kramer, E. J.; Berger, L. L. *Adv. Polym. Sci.* **1990**, *91/92*, 1.
43. Estevez, R.; Tijssens, M. G. A.; Van der Giessen, E. *J. Mech. Phys. Solids* **2000**, *48*, 2585.
44. Kulikovm O.; Hornung, K.; Wagner, H. M. *Rheol. Acta* **2007**, *46*, 741.
45. Brochard, F.; de Gennes, P.-G. *Langmuir* **1992**, *8*, 3033.
46. Allal, A.; Lavernhe, A.; Vergnes, B.; Marin, G. *J. Non-Newtonian Fluid Mech.* **2006**, *134*, 127.
47. Allal, A.; Vergnes, B. *J. Non-Newtonian Fluid Mech.* **2007**, *146*, 45.
48. Yamaguchi, M.; Miyata, H.; Tan, V.; Gogos, C. G. *Polymer* **2002**, *43*, 5249.
49. Carreau, P. J. PhD thesis, University of Wisconsin. **1968**.
50. Mieda, N.; Yamaguchi, M. *J. Non-Newtonian Fluid Mech.* **2011**, *166*, 231.
51. Suzuki, M.; Ali, M. A. M.; Okamoto, K.; Taniike, T.; Terano, M.; Yamaguchi, M. *Adv. Polym. Tech.* **2009**, *28*, 185.